

Antineutrino geophysics with liquid scintillator detectors

Casey G. Rothschild, Mark C. Chen and Frank P. Calaprice

Physics Department, Princeton University Princeton, New Jersey

arXiv:nucl-ex/9710001v2 1 Jun 2005

Short title: ANTINEUTRINO GEOPHYSICS WITH LIQUID SCINTILLATOR
DETECTORS

Abstract. Detecting the antineutrinos emitted by the decay of radioactive elements in the mantle and crust could provide a direct measurement of the total abundance of uranium and thorium in the Earth. In calculating the antineutrino flux at specific sites, the local geology of the crust and the background from the world's nuclear power reactors are important considerations. Employing a global crustal map, with type and thickness data, and using recent estimates of the uranium and thorium distribution in the Earth, we calculate the antineutrino event rate for two new neutrino detectors. We show that spectral features allow terrestrial antineutrino events to be identified above reactor antineutrino backgrounds and that the uranium and thorium contributions can be separately determined.

Introduction

The possibility to study the radiochemical composition of the Earth by detecting, at the surface, the antineutrinos ($\bar{\nu}_e$) emitted by the decay of radioactive isotopes within has been suggested before [Eders, 1966; Marx, 1969; Marx and Lux, 1970; Avilez et al., 1981; Krauss et al., 1984; Kobayashi and Fukao, 1991]. Confirming the abundance of certain radioactive elements in the crust and mantle could establish important geophysical constraints on the heat generation within the Earth. Radioactivity is thought to be the dominant heat source driving mantle convection [Davies and Richards, 1992; Sleep, 1990]. It is also an important factor in determining the surface heat flow in continents and in understanding the thermal history of the Earth. Uranium and thorium, in particular, play an important role due to their relatively large abundances and long half-lives. Improved constraints on the present uranium and thorium abundances in the mantle and crust could yield better estimates for these internal, geodynamic heat sources.

Detecting the low-energy antineutrinos from radioactivity is a challenge due to their small interaction cross-section. At present, the only practical medium for detecting terrestrial antineutrinos would be a large-mass liquid scintillator, observing the inverse β -decay reaction on the proton. New scintillator detectors are being built in Italy and Japan that could inaugurate the field of antineutrino geophysics.

Various candidates for the target nucleus to be used in an antineutrino detector have also been discussed; however, if practical considerations for procuring the huge

quantities (tons) of target material are evaluated, only hydrogen, in the form of water or organic liquid scintillator (CH_2), emerges as a feasible target. The reaction:

$$\bar{\nu}_e + p \rightarrow e^+ + n, \quad (1)$$

has a relatively large cross-section. Its main advantage is the production of a neutron which captures with a mean lifetime of about $200 \mu\text{s}$, via $n + p \rightarrow d + \gamma$, releasing 2.2 MeV energy and forming a delayed coincidence with the positron. This provides a distinctive event signature for an antineutrino interaction. The threshold for this reaction is 1.8 MeV; the maximum energy of the antineutrinos produced by natural radioactivity is 3.27 MeV. Consequently, the positron from (1) deposits at most 2.5 MeV (including both 0.511 MeV annihilation γ rays). At these low energies, liquid scintillator detectors would be favored over water Čerenkov detectors, due to their higher light yield.

Of the naturally-occurring radioactive elements in the Earth, only four β decays in the ^{238}U and ^{232}Th chains produce a significant number of antineutrinos with energy greater than 1.8 MeV. The decay of ^{214}Bi (U chain) has an 18% branch [*Lederer and Shirley, 1978*] to the ground state, with a β endpoint of 3.27 MeV. The β decays from ^{234}Pa (U chain), ^{228}Ac and ^{212}Bi (Th chain) have practically the same maximum decay energy, 2.29 MeV, 2.08 MeV, and 2.25 MeV, respectively. Consequently, the terrestrial $\bar{\nu}_e$ spectrum above 1.8 MeV takes on a “two-component” form, with its higher-energy component coming solely from ^{238}U decay and a lower component with contributions from ^{238}U and ^{232}Th . This distinctive spectral shape would also assist in identifying

these events in a scintillation detector.

Uranium and Thorium Distribution

It is usually assumed that the Earth's core contains no U and Th after core/mantle partitioning [Kargel and Lewis, 1993]. Consequently, the starting point for determining the distribution of uranium and thorium in the present crust and mantle is understanding the composition of the "Bulk Silicate Earth" (BSE), which is the model representing the primordial mantle prior to crust formation (equivalent in composition to the modern mantle plus crust). BSE compositional estimates have been compiled [Kargel and Lewis, 1993] and derived using several techniques. More recently, BSE concentrations of 0.0795 ppm ($\pm 15\%$) for ^{232}Th and 0.0203 ppm ($\pm 20\%$) for U, have been suggested [McDonough and Sun, 1995], with subjective error estimates that encompass most of the values listed in [Kargel and Lewis, 1993]. This amount of thorium in the mantle and crust would produce 9 TW of heat, and uranium 8 TW, which can be compared to the total global heat outflow of ~ 40 TW [Davies, 1980; Sclater et al., 1980].

In the formation of the Earth's crust, the primitive mantle was depleted of uranium and thorium [O'Nions and McKenzie, 1993], while the continental crust, in particular, was highly enriched [Plant and Saunders, 1996]. Rock samples from the upper continental crust provide direct isotopic abundance information. Data from continental heat flow measurements [Pollack and Chapman, 1977] are also important in deducing the bulk radiochemical composition. A recent perspective on the nature of the continental crust [Rudnick and Fountain, 1995] includes data from chemical studies

of lower crustal rocks and makes lithological assignments from seismological data to improve estimates of the composition of the middle and lower crust. Combining these sources, the current best estimates for the average uranium and thorium concentrations in the continental crust are listed in Table 1.

Table 1

Samples of mid-ocean ridge basalts (MORB) provide the main input for estimating the bulk uranium and thorium content of oceanic crust. Concentrations slightly higher than those found in typical MORB's are representative of the bulk oceanic crust composition [Jochum *et al.*, 1983; Taylor and McLennan, 1985]; values are listed in Table 1.

With the above data, the average U and Th concentrations for the “residual”, present-day mantle can be calculated. We assumed an average thickness of 40 km for the continental crust [Taylor and McLennan, 1985] and 6 km for the oceanic crust [Taylor and McLennan, 1985] and subtracted these enriched layers from the BSE concentrations. An interesting problem is distributing the isotopic depletion of the mantle. The discontinuity at 670 km depth may act as a barrier to mass flow [Ringwood and Irifune, 1988], resulting in U and Th depletion of only the upper mantle. Others do not consider this to be the case [Christensen, 1989]. Taking the assumption of whole-mantle convection, we selected a uniform composition for the entire mantle and list average U and Th concentrations in Table 1.

Results

The difference in U and Th activity between continental and oceanic crust is substantial. Therefore, the crustal topography near an antineutrino detector is important to take into account when calculating the $\bar{\nu}_e$ flux; previous calculations did not include such a detailed analysis. We employed crust type and thickness data in the form of a global crustal map: (W. D. Mooney, G. Laske, and T. G. Masters, CRUST 5.1: A Global Crustal Model at $5^\circ \times 5^\circ$, submitted to the *Journal of Geophysical Research*, 1997; data accesible from the World Wide Web server for the U.S. Geological Survey at <http://quake.wr.usgs.gov/study/CrustalStructure/>). The data include 16 primary crust types with about 140 different sub-types. In our calculations, we lumped the crust classification into just continental and oceanic and used the average U and Th concentrations (from Table 1) regardless of sub-classification, but did use the crust thickness data, which range from 6–70 km.

We calculated the $\bar{\nu}_e$ flux from U and Th decay for several sites around the world. In the ^{238}U decay chain, there are 6 β decays ($\bar{\nu}_e$ emitting) for each ^{238}U decay; the ^{232}Th decay chain goes through 4 β decays per ^{232}Th decay. In Table 2, these factors were included in the tabulated fluxes. From this total flux only an average of 0.38 antineutrinos per ^{238}U decay (from all branches in the entire decay chain) have energy above the reaction threshold of 1.804 MeV. For the thorium chain, an average of 0.15 antineutrinos per ^{232}Th decay can make the inverse β -decay reaction.

Table 2

Entries for the geographic “maximum” and “minimum” are also included in Table 2.

In these two bounding, hypothetical cases, the maximum refers to the situation where all of the continental crust (of average thickness 40 km, covering 40% of the Earth's surface area) forms a circular cap centered around the $\bar{\nu}_e$ detector. The minimum refers to the contrasting scenario, with a $\bar{\nu}_e$ detector in the middle of a grand ocean (6 km oceanic crust covering 60% of the Earth). It is interesting that the terrestrial $\bar{\nu}_e$ flux for a site in the Himalayas is close to the geographic maximum flux; this is due to a crust thickness of ~ 70 km in this region, which exceeds the average value.

To lowest-order, neglecting the neutron recoil, the cross-section for $\bar{\nu}_e$ capture on protons is [Vogel, 1984]:

$$\sigma(E_\nu) = \frac{2\pi^2 \hbar^3}{m_e^5 c^8 f\tau_n} (E_\nu - \Delta Mc^2) [(E_\nu - \Delta Mc^2)^2 - (m_e c^2)^2]^{1/2}, \quad (2)$$

where ΔM is the neutron-proton mass difference, and the $f\tau_n$ values come from neutron β decay [Wilkinson, 1982; Particle Data Group, 1996]. We integrated this cross-section with the antineutrino spectra from each energetic U and Th β decay, including Fermi function corrections [Behrens and Jänecke, 1969], to estimate event rates in two new liquid scintillator detectors being built. The Borexino experiment at Gran Sasso will contain 280 tons of pseudocumene-based scintillator (C_9H_{12}); in this detector, the terrestrial antineutrino event rate would be 10 events per year. For the Kam-LAND experiment in the Kamioka mine, 1,000 tons of mineral-oil-based scintillator (CH_2-) would detect 29 $\bar{\nu}_e$ events from U and Th decay per year.

Discussion

The terrestrial $\bar{\nu}_e$ event rates are very low; however, these events have a correlated signature, the positron–neutron delayed coincidence. The most problematic background in reactor antineutrino experiments are fast neutrons (especially those produced by muon interactions). To minimize this background requires: an underground location for cosmic-ray flux reduction; low-radioactivity in the detector; sufficient external neutron shielding; and a tight muon veto surrounding the detector. These conditions might be satisfied in the two new experiments.

A background that cannot be shielded is the $\bar{\nu}_e$ flux from the world’s nuclear reactors [Lagage, 1985]. In Table 2, we also list our calculated reactor $\bar{\nu}_e$ fluxes. This calculation employed data from the International Nuclear Safety Center Database and assumed all reactors operating at full power (data for all of the world’s nuclear reactors are available from the World Wide Web server for the International Nuclear Safety Center at <http://www.insc.anl.gov>). The scaling of the $\bar{\nu}_e$ flux was based upon a reactor antineutrino yield of 5×10^{20} $\bar{\nu}_e$ per second for 2,800 MW thermal power [Zacek et al., 1986] and a typical efficiency of 33% for electric/thermal power.

The unique two-component shape of the terrestrial antineutrino energy spectrum makes it possible to identify these events above the reactor $\bar{\nu}_e$ background. In Figure 1, the energy spectrum for the positrons produced by $\bar{\nu}_e$ capture on protons is displayed, revealing spectral features at 1.5 and 2.5 MeV. The positron spectrum from reactor antineutrinos has a well-known shape [Zacek et al., 1986]. Measuring this spectrum

Figure 1

enables the reactor backgrounds to be subtracted and allows the higher-energy terrestrial $\bar{\nu}_e$ component from uranium to be separated from the thorium contribution.

Site selection would be important for future terrestrial $\bar{\nu}_e$ experiments. A site in Australia, far from any nuclear reactors, has a flux $\sim 200\times$ lower than the reactor $\bar{\nu}_e$ flux at Kamioka. An oceanic location (possibly near Hawaii) enables a $\bar{\nu}_e$ flux measurement to be predominantly sensitive to radioactivity from the mantle. It would be interesting to compare the terrestrial antineutrino data from several experiments around the world. In doing so, one might be able to separate the contributions from the crust and mantle. Though event rates will be low and background suppression a challenge, two new experiments will be evaluating these backgrounds and exploring the prospects for antineutrino geophysics in the near future.

Acknowledgments. We thank Profs. F. A. Dahlen, K. S. Deffeyes and T. S. Duffy, from the Department of Geosciences, Princeton University, for useful discussions and Prof. A. Suzuki for providing information about the Kam-LAND experiment.

References

- Avilez, C., G. Marx and B. Fuentes, Earth as a source of antineutrinos, *Phys. Rev. D*, **23**, 1116–1117, 1981.
- Behrens, H., and J. Jänecke, *Numerical Tables for Beta-Decay and Electron Capture*, 316 pp., Springer-Verlag, Berlin, 1969.
- Christensen, U. R., Models of mantle convection: One or several layers, *Phil. Trans. R. Soc. Lond.*, **328**, 417–424, 1989.
- Davies, G. F., Thermal histories of convective Earth models and constraints on radiogenic heat production in the Earth, *J. Geophys. Res.*, **85**, 2517–2530, 1980.
- Davies, G. F., and M. A. Richards, Mantle convection, *J. Geol.*, **100**, 151–206, 1992.
- Eders, G., Terrestrial neutrinos, *Nucl. Phys.*, **78**, 657–662, 1966.
- Jochum, K. P., A. W. Hoffman, E. Ito, H. M. Seufert, and W. M. White, K, U and Th in mid-ocean ridge basalt glasses and heat production, K/U and K/Rb in the mantle, *Nature*, **306**, 431–436, 1983.
- Kargel, J. S., and J. S. Lewis, The composition and early evolution of Earth, *Icarus*, **105**, 1–25, 1993.
- Krauss, L. M., S. L. Glashow, and D. N. Schramm, Antineutrino astronomy and geophysics, *Nature*, **310**, 191–198, 1984.
- Kobayashi, M., and Y. Fukao, The Earth as an antineutrino star, *Geophys. Res. Lett.*, **18**, 633–636, 1991.

- Lagage, P. O., Nuclear power stations as a background source for antineutrino astronomy, *Nature*, **316**, 420–421, 1985.
- Lederer, C. M., and V. S. Shirley (Eds.), *Table of Isotopes, Seventh Edition*, 1523 pp., John Wiley, New York, 1978.
- Marx, G., Geophysics by neutrinos, *Czech. J. Phys. B*, **19**, 1471–1479, 1969.
- Marx, G., and I. Lux, Hunting for soft antineutrinos, *Acta Phys. Acad. Sci. Hung.*, **28**, 63–70, 1970.
- McDonough, W. F., and S.-s. Sun, The composition of the Earth, *Chem. Geol.*, **120**, 223–253, 1995.
- O’Nions, R. K., and D. McKenzie, Estimates of mantle thorium/uranium ratios from Th, U and Pb isotope abundances in basaltic melts, *Phil. Trans. A*, **342**, 65–77, 1993.
- Particle Data Group, Review of Particle Physics, *Phys. Rev. D*, **54**, 1–720, 1996.
- Plant, J. A., and A. D. Saunders, The radioactive Earth, *Radiation Protection Dosimetry*, **68**, 25–36, 1996.
- Pollack, H. N., and D. S. Chapman, On the regional variation of heat flow, geotherms, and lithospheric thickness, *Tectonophysics*, **38**, 279–296, 1977.
- Ringwood, A. E., and T. Irifune, Nature of the 650 km seismic discontinuity: Implications for mantle dynamics and differentiation, *Nature*, **331**, 131–137, 1988.
- Rudnick, R. L., and D. M. Fountain, Nature and composition of the continental crust: A lower crustal perspective, *Rev. Geophys.*, **33**, 267–309, 1995.

Sclater, J. G., C. Jaupart, and D. Galson, The heat flow through oceanic and continental crust and the heat loss of the Earth, *Rev. Geophys. Space Sci.*, **18**, 269–311, 1980.

Sleep, N. H., Hotspots and mantle plumes: Some phenomenology, *J. Geophys. Res.*, **95**, 6715–6736, 1990.

Taylor, S. R., and S. M. McLennan, *The Continental Crust: its Composition and Evolution*, 312 pp., Blackwell Scientific, Oxford, 1985.

Vogel, P., Analysis of the antineutrino capture on protons, *Phys. Rev. D*, **29**, 1918–1922, 1984.

Wilkinson, D. H., Analysis of neutron β -decay, *Nucl. Phys. A*, **377**, 474–504, 1982.

Zacek, G. *et al.*, Neutrino-oscillation experiments at the Gösgen nuclear power reactor, *Phys. Rev. D*, **34**, 2621–2636, 1986.

F. P. Calaprice, M. C. Chen and C. G. Rothschild, Physics Department, Princeton University, Princeton, New Jersey 08544. (e-mail: fpc@pupcyc2.princeton.edu; mchen@post.queensu.ca; caseyr@princeton.edu)

Received September 23, 1997; revised February 10, 1998; accepted February 18, 1998.

Published in *Geophysical Research Letters*, **25**, 1083 (1998).

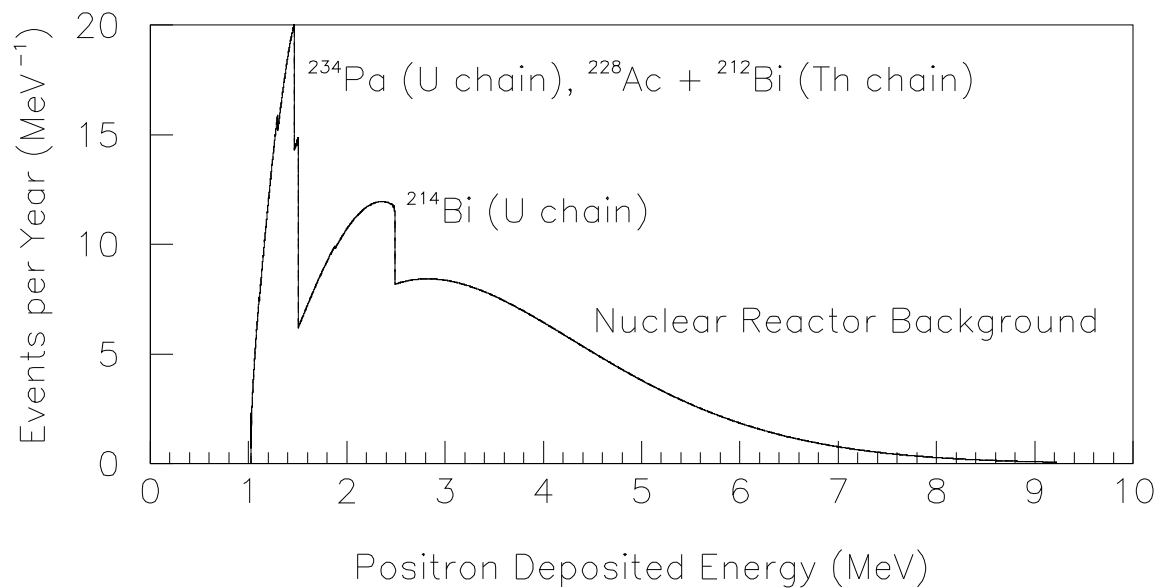


Figure 1. Positron energy spectrum from $\bar{\nu}_e$ events in a 280-ton detector at the Gran Sasso underground laboratory. The reactor $\bar{\nu}_e$ background rate is 29 events per year, with only 7.6 events in the same spectral region as the terrestrial antineutrinos.

Table 1. Uranium and thorium abundances in the Earth.

	$[^{238}\text{U}]$ in ppm	$[^{232}\text{Th}]$ in ppm
Bulk Silicate Earth [<i>McDonough and Sun, 1995</i>]	0.0203	0.0795
average continental crust [<i>Rudnick and Fountain, 1995</i>]	1.4	5.6
average oceanic crust [<i>Taylor and McLennan, 1985</i>]	0.10	0.22
present-day “residual” mantle	0.013	0.052

Table 2. Calculated $\bar{\nu}_e$ fluxes [$\times 10^6 \text{ cm}^{-2} \text{ s}^{-1}$] for sites around the world.

Site	Location	Uranium		Thorium		Total	Reactor
		crust	mantle	crust	mantle	(U + Th)	background
Gran Sasso Lab (Italy)	42°N 14°E	2.5	1.2	2.2	1.0	6.9	0.65
Kamioka Mine (Japan)	36°N 137°E	0.82	1.2	0.69	1.0	3.7	3.7
Sudbury (Canada)	47°N 81°W	3.2	1.2	2.8	1.0	8.2	1.3
Central Australia	25°S 133°E	2.7	1.2	2.4	1.0	7.3	0.016
Himalayas (Tibet)	33°N 85°E	3.5	1.2	3.1	1.0	8.8	0.054
Pacific Ocean (Hawaii)	20°N 156°W	0.30	1.2	0.23	1.0	2.7	0.027
Geographic Maximum		3.5	1.2	3.1	1.0	8.8	
Geographic Minimum		0.21	1.2	0.16	1.0	2.6	